Medicine®

OBSERVATIONAL STUDY

OPEN

Posttransplant Lymphoproliferative Disorder of the Thorax: CT and FDG-PET Features in a Single Tertiary Referral Center

Ga Young Yoon, MD, Mi Young Kim, MD, PhD, Joo Rryung Huh, MD, PhD, Kyung-Wook Jo, MD, PhD, and Tae Sun Shim, MD, PhD

Abstract: To investigate the chest computed tomography (CT) and F-18 fluoro-2-deoxy-D-glucose positron emission tomographic (FDG-PET) findings of posttransplant lymphoproliferative disorder (PTLD) in the thorax.

From November 2004 to February 2013, the cases of 12 adult patients (3 female and 9 male, age range 34–68, and median age 46 years) with proven PTLD were retrospectively reviewed. The transplanted organs included the kidney (5/12), liver (4/12), heart (1/12), combined kidney and pancreas (1/12), and hematopoietic stem cell (1/12). We investigated the relationship of the Epstein–Barr virus (EBV) to the patients' long-term follow-up, and evaluated the characteristics of the lesions on the chest CT and FDG-PET. The lesions were classified into 2 patterns: that of lymph node and lung involvement.

The interval between the transplantation and the onset of PTLD was 2 to 128 months (median, 49). Positive EBV-encoded RNA in the pathologic specimens was found in 10 patients (83.3%). Eight patients were positive for EBV PCR in their blood, and 3 patients showed seroconversion without antiviral therapy. The responses to treatment were complete in 7 cases (58.3%), partial remission in 4 cases (33.3%), and undetermined in 1 case (8.3%). The more common chest CT patterns showed lymph node involvement (10/12) rather than lung involvement (3/12). The median maximum-standardized uptake value on the FDG-PET scans was 7.7 (range, 2.7–25.5).

In patients with PTLD involving the thorax, lymphadenopathy was the more common manifestation on the chest CT rather than lung involvement. The lesions showed hypermetabolism on FDG-PET.

(*Medicine* 94(31):e1274)

Abbreviations: CT = computed tomography, EBV = Epstein–Barr virus, FDG-PET = F-18 fluoro-2-deoxy-D-glucose positron emission tomography, LN = lymph node, PTLD = posttransplant lymphoproliferative disorder, SUVmax = maximum-standardized uptake value.

INTRODUCTION

Posttransplant lymphoproliferative disorder (PTLD) is a family of disorders that include lymphoid hyperplasia and lymphoid neoplasia. It occurs in the setting of immunosuppression after transplantation. The majority of PTLDs involve B cell proliferation and related Epstein–Barr virus (EBV) infection, because the EBV-infected B cells proliferate when the T cells are depleted due to therapeutic immunosuppression.[1–3] In 1968, Starzl described PTLD in renal transplant recipients.[4]

The incidence of PTLD varies according to several factors that include the patient's age, the EBV status at the time of the transplantation, the donor source (living or nonliving), and the immunosuppressive regimen. The clinical manifestations of PTLD commonly include mononucleosis-type syndrome (ie, fever, fatigue, and sore throat), regional lymphoid tumors, and a disseminated disease.[5] It is very difficult to diagnose without a history of posttransplantation and histology confirmation. Because the symptoms of PTLD are often similar to those of other complications of transplantation, particularly infection and organ rejection, a high index of PTLD suspicion is crucial to preventing a delay in diagnosis. PTLD is a challenging complication of organ transplantation and if left untreated, is often fatal.[4]

As PTLD that affects the thorax is rare, its chest computed tomography (CT) characteristics are not yet well-established. In this paper, the chest CT imaging and F-18 fluoro-2-deoxy-D-glucose positron emission tomographic (FDG-PET) characteristics of thoracic PTLD observed in 12 adult patients in a single tertiary referral center, and the results of their long-term follow-up are reported. The imaging features may provide some diagnostic clues for radiologists to consider the possibility of this condition in patients with organ transplants.

MATERIALS AND METHODS

Patient Characteristics

From April 1992 to December 2012, 8000 patients older than 18 years consecutively underwent organ (7090/8000) or hematopoietic stem cell (910/8000) transplantation at our tertiary referral hospital. PTLD was later diagnosed in 34 of these patients, which represents a 0.4% frequency (34/8000). The patients who have had autologous transplantations (n = 20) were initially excluded. Then from among the cases of the 34 patients, the PTLD cases that involved various other organs were excluded (22/34). Finally, solid organ (11/12) and hematopoietic stem cell (1/12) transplantations in 12 of the 34 patients (35.3%) with thoracic involvement were included in this study (Figure 1). The study group consisted of 12 patients (9 men and 3 women). They underwent the following transplantations: 1 combined kidney and pancreas transplantation, and 5 kidney, 4 liver, 1 heart, and 1 hematopoietic stem cell

Editor: Lydia Eccersley.
Received: March 2, 2015; revised: July 1, 2015; accepted: July 8, 2015.
From the Department of Radiology and Research Institute of Radiology (GYY, MYK); Department of Pathology (JRH); and Department of Pulmonary and Critical Care Medicine, University of Ulsan College of Medicine, Asan Medical Center, Seoul, South Korea (KWJ, TSS).
Correspondence: Mi Young Kim, Department of Radiology and Research Institute of Radiology, University of Ulsan College of Medicine, Asan Medical Center, 86 Asanbyeongwon-Gil, Songpa-Gu, Seoul 138-736, South Korea (e-mail: mimowdr@amc.seoul.kr).
The authors have no funding and conflicts of interest to disclose.

ISSN: 0025-7974
DOI: 10.1097/MD.0000000000001274

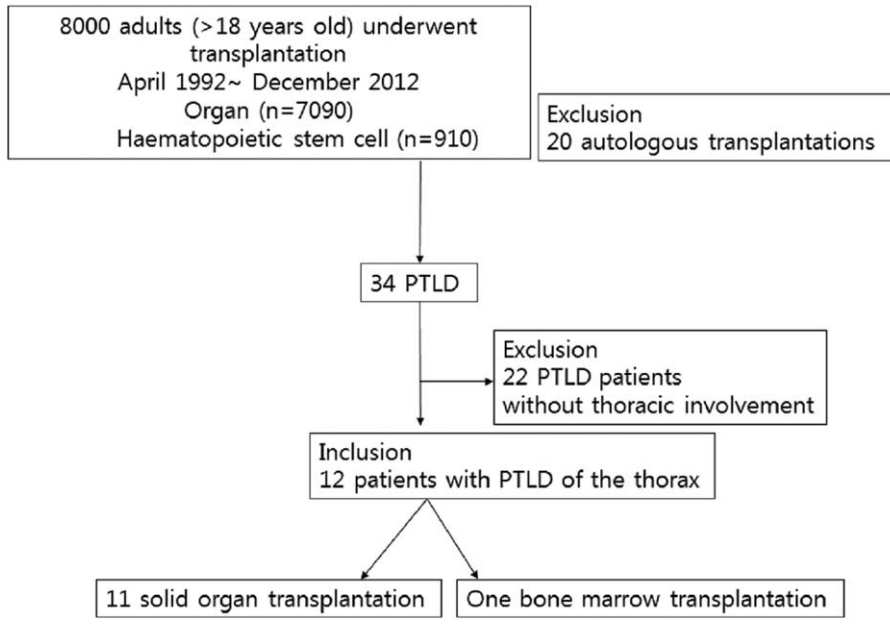

FIGURE 1. Patients' inclusion criteria.

transplantation. The median patient age at the time of the transplantation was 40 years (range, 28–68 years).

This retrospective study was approved by the Institutional Review Board of Asan Medical Center. The patients' informed consent was waived (Institutional Review Board reference number 2013–1097).

Diagnosis of PTLD and EBV Infection

The PTLD diagnosis was histopathologically established during the examination of the core biopsy material or the excision in all the patients (Figures 2–4). The core biopsy was performed using an 18-gauge, double-action, and spring-activated needle (Ace-cut; Create Medic, Yokohama, Japan). The tissue samples were reviewed by a pathologist (JH, with 22 years of experience in pathology as a hematologic malignancy specialist) and classified according to the World Health Organization classification.

To determine the frequency of EBV infection in the tissue affected by PTLD, in situ hybridization to identify Epstein–Barr virus-encoded RNA (EBER) was performed on all the specimens. Also, all the patients underwent an EBV polymerase chain reaction (PCR) test of their blood at the time of their diagnosis; and among them, 3 cases were subjected to routine EBV PCR monitoring for posttransplant surveillance.

CT Scanning Protocol

Various generations of CT scanners were used in this study (for a total of 12 CT scans). The most representative chest CT examinations were performed using SOMATOM (Siemens Medical Solutions, Forchheim, Germany) (8 patients) or Lightspeed volume computed tomography (VCT) (General Electric Medical Systems, Milwaukee, WI) (4 patients). The SOMATOM scanner was used with a 120 kV peak and 100 effective mAs with dose modulation. The reconstruction intervals were 3 to 5 mm thick and had no gap for the B50 algorithm, and were 1 mm thick with a 5 mm gap for the B60 algorithm. The General Electric CT scanner was used with the following parameters: a 120 kV peak and 100 to 300 mA with dose modulation. The reconstruction intervals were 2.5 to 5 mm thick and had no gap for the lung algorithm, and were 1.25 mm thick with a 5 mm gap for the bone algorithm. All the CT images were routinely reformatted on a coronal plane.

The scan range was from the supraclavicular area to the level of the adrenal glands. The CT contrast and 50 mL normal saline were injected at a rate of 2.5 mL/seconds using a power injector. All the images were viewed on the mediastinal axial image setting (width, 450 HU and level, 50 HU) and the lung window axial image setting (width, 1500 HU and level, −700 HU) in the picture archiving and communication system.

CT Evaluation

Two radiologists (MYK with 18 years of experience in thoracic radiology and GYY with 3 years of experience in radiology) who were blinded to the clinical data, except to the fact that the patients had PTLD, interpreted the 12 chest CT images in consensus.

The locations and characteristics of the imaging abnormalities seen on the chest CT (12/12) were evaluated. The lesions were classified into lymph nodes (LNs) and lung involvement according to their different patterns (Table 3). The pleural lesion was evaluated as an ancillary finding.

The LN involvement was evaluated based on the following factors: the location according to the nodal station of the TNM stage,[6] bilaterality, number of lesions, size of the largest node in the short-access diameter (>5 mm) with clustering (more than 3), attenuation (HU), and heterogeneity compared to the adjacent muscle. The lung involvement was analyzed according to the location, numbers of lesions, size of the lesion's longest diameter, attenuation, and heterogeneity

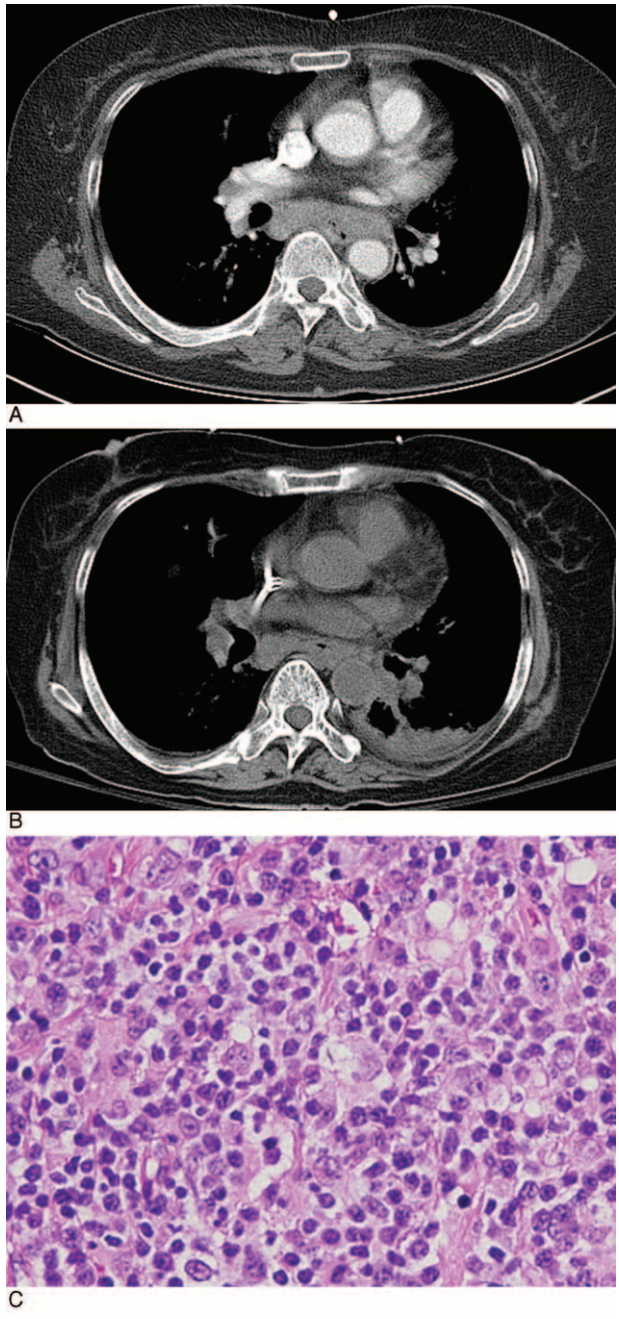

FIGURE 2. A 61-year-old woman who developed PTLD of the thorax 3 months after hematopoietic stem cell transplantation (patient 7). (A) Contrast-enhanced axial CT image obtained at the level of the aortic root, showing a short 19 mm diameter and a homogenous nodal mass both in the subcarinal and paraesophageal areas. (B) Follow-up CT scan obtained 2 months later showing partial resolution of the nodal masses after immune therapy and chemotherapy. (C) Histopathology of the left axillary lymph node revealing a monomorphic PTLD of the peripheral T-cell type, as well as composed of unspecified medium-sized cells with a clear cytoplasm (Hematoxylin-Eosin stain; 400× magnification). CT = computed tomography, PTLD = posttransplant lymphoproliferative disorder.

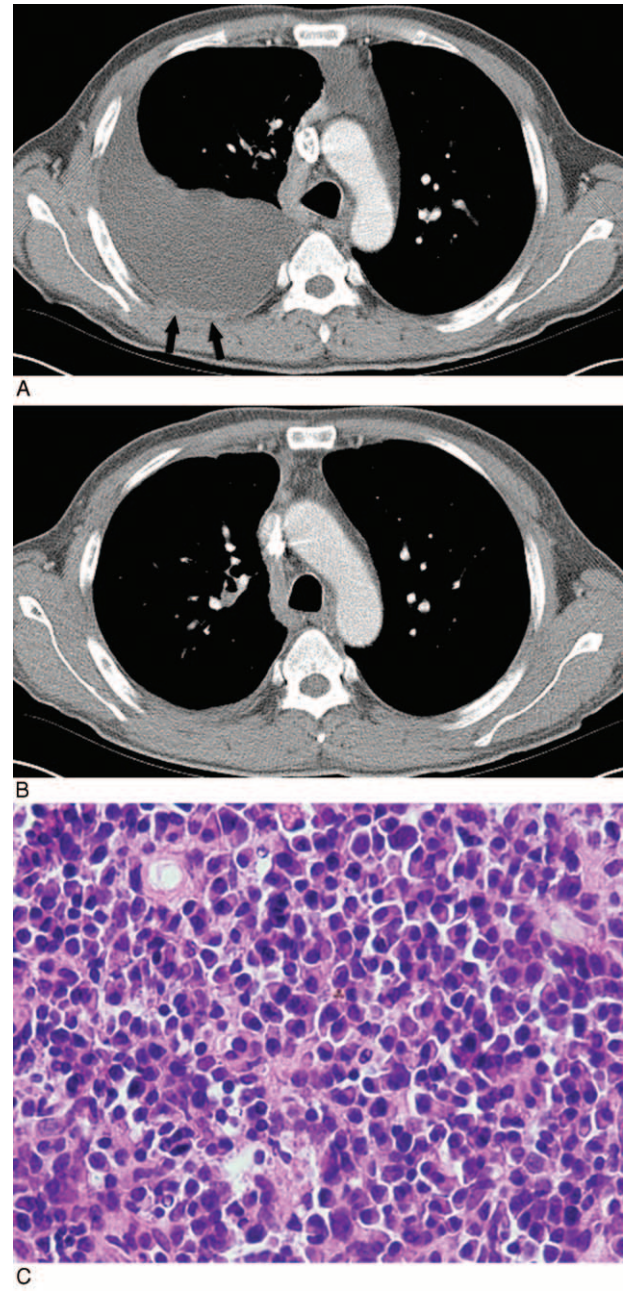

FIGURE 3. A 42-year-old man who developed PTLD of the thorax 5 years and 1 month after kidney transplantation (patient 9). (A) Contrast-enhanced axial CT image obtained at the level of the aortic arch showing right pleural effusion with enhanced mild and diffuse pleural thickening (arrow). (B) Follow-up CT scan obtained a month later showing a decreased amount of right pleural effusion and no pleural thickening after immune therapy and chemotherapy. (C) Lymph node biopsy showing a monomorphic PTLD, or a plasmacytoma composed of plasma cells with characteristic eccentric nuclei (Hematoxylin-Eosin stain; 400× magnification). CT = computed tomography, PTLD = posttransplant lymphoproliferative disorder.

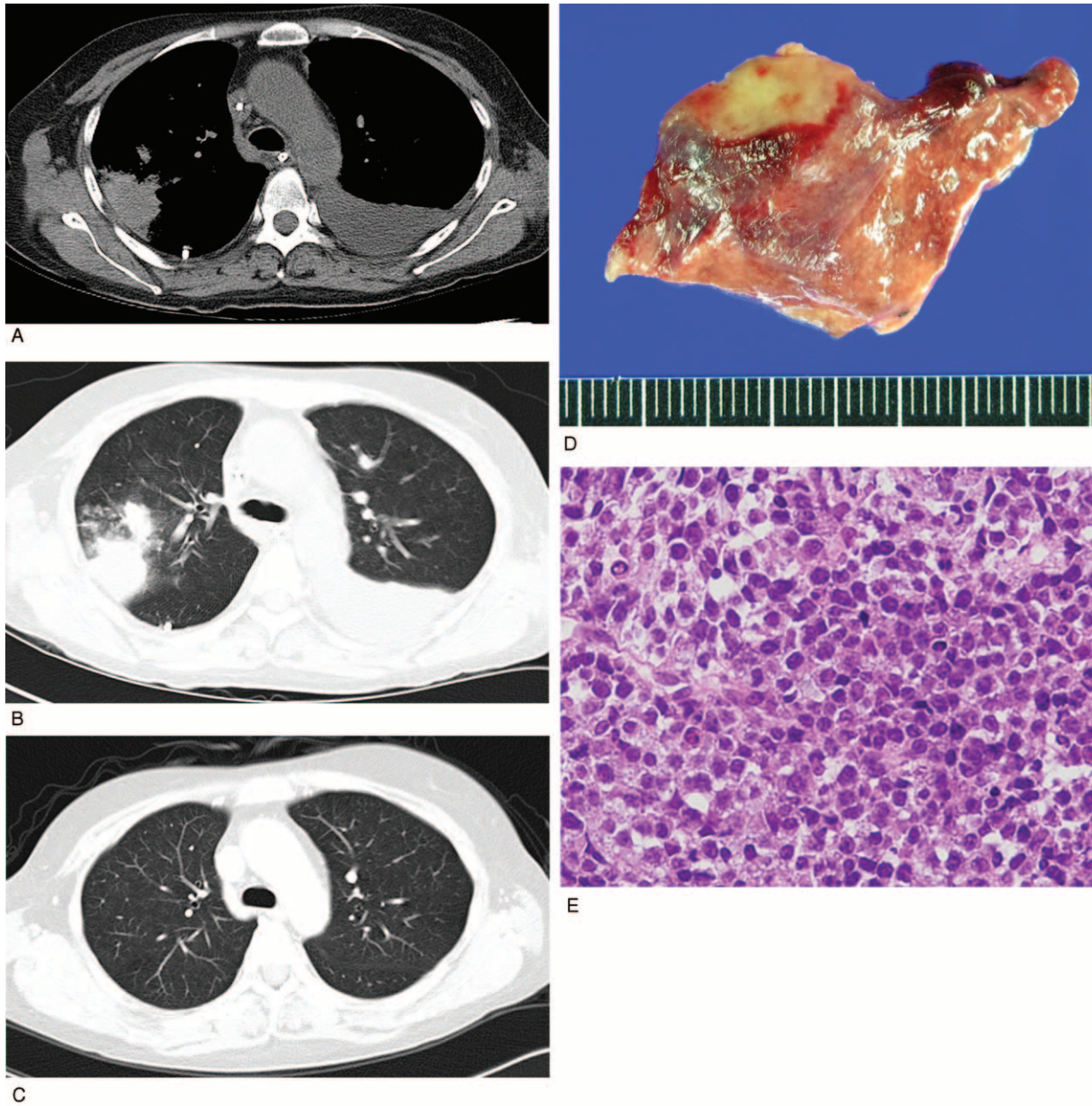

FIGURE 4. A 35-year-old woman who developed PTLD of the thorax 15 months after kidney transplantation (patient 5). (A, B) Nonenhanced axial CT images in the mediastinal and lung window images obtained at the level of the aortic arch, showing a 4 cm ill-defined, mass-like consolidation with surrounding ground-glass opacity in the right upper lobe. Note also the left pleural effusion. (C) Follow-up CT scan obtained 15 months later showing complete resolution of the mass after surgical resection and immune therapy and chemotherapy. (D) Photograph after pulmonary wedge resection of a mass showing a soft, gelatinous, tan, and fish-flesh-like cut surface. (E) Microscopically, lesions showing monomorphic PTLD of the diffuse large B-cell type and composed of sheets of large tumor cells of B-cell lineage (Hematoxylin-Eosin stain; 400× magnification). CT = computed tomography, PTLD = posttransplant lymphoproliferative disorder.

compared to the adjacent muscle, as well as according to the presence of necrotic lower attenuation. The presence of pleural effusion and laterality when the pleural effusion was improving after the treatment, and the high 18F-fluorodeoxy glucose PET/CT uptake (>2.5 maximum-standardized uptake value [SUVmax]) was simultaneously described.

FDG-PET Scanning Protocol

The FDG-PET was obtained using a commercially available machine (Discovery PET/CT 690; GE Health Care, Wisconsin) (>2.5 times the SUVmax). The mean interval between the CT and FDG-PET studies was 9.2 ± 8.6 days. On the FDG-PET scans, the 3 highest SUVmax values of the lesions were obtained, and the median value per patient was calculated.

TABLE 1. Clinical Characteristics in 12 Patients with Posttransplantation Lymphoproliferative Disorder of the Thorax

Patient No./Age (year)/ Sex	C/C	Smoker	Transplant	Pretransplantation	Time Before PTLD, month*	Pathologic Type	EBV ISH†	EBV Titer, copies/mL‡	Seroconversion	Therapy	Response of Therapy	Follow-Up, month
1/35/M	Fever	−	Kidney, Pancreas	Diabetic neuropathy	22	Monomorphic DLBCL	+	102,500	No FU	Surgery, RI, CTx (R-CHOP)	CR	37
2/60/M	−	−	Liver	HCC/LC	14	Monomorphic DLBCL	+	<1000	No FU	RI, CTx (R-CHOP)	PR	9
3/40/M	Fever	−	Heart	DCMP	128	Monomorphic PTCL, NOS	+	243,250	No FU	RI, CTx (CHOP)	CR	17
4/44/M	Palpable neck mass	−	Kidney	CRF	94	Monomorphic DLBCL	−	Undetectable	No FU	RI, CTx (R-CHOP)	PR	16
5/35/F	Fever	−	Kidney	CRF	15	Monomorphic DLBCL	+	367,500	+	Surgery, RI, CTx (R-CHOP)	CR	12
6/54/F	−	−	Liver	HCC/LC	9	Polymorphic	+	40,250	No FU	RI, CTx (CHOP)	CR	13
7/62/F	−	−	Bone marrow	AML	3	Monomorphic PTCL, NOS	+	822,500	+	RI, CTx (Rituximab)	PR	2
8/48/M	−	−	Liver	Cirrhosis	2	Monomorphic DLBCL	+	Undetectable	No FU	Unknown§	Unknown§	0
9/34/M	Fever	−	Kidney	CRF (HTN)	61	Monomorphic Plasmacytoma	−	Undetectable	No FU	RI, CTx (CHOP)	CR	62
10/68/M	−	−	Liver	HCC/LC	7	Monomorphic DLBCL	+	28,500	+	RI, CTx (R-CHOP)	CR	8
11/44/M	Anorexia	+	Kidney	ESRD	117	Monomorphic DLBCL	+	Undetectable	No FU	RI, CTx (R-CHOP)	CR	66
12/54/M	−	−	Kidney	ESRD	114	Monomorphic DLBCL	+	57,250	No FU	Surgery, RI, CTx (R-CHOP)	PR	3

AML = acute myeloid leukemia, CHOP = cyclophosphamide, doxorubicine, vincristine, and prednisolone, CR = complete remission, CRF = chronic renal failure, CTx = chemotherapy, DCMP = di-dilated cardiomyopathy, DLBCL = diffuse large B-cell lymphoma, ESRD = end stage renal disease, HCC/LC = hepatocellular carcinoma with cirrhosis, LN = lymph node, NOS = not otherwise specified, PR = partial remission, PTCL = peripheral T-cell lymphoma, R-CHOP = rituximab, cyclophosphamide, doxorubicine, vincristine, and prednisolone, RI = reduced immunosuppression.

* Time between transplantation and the development of PTLD.

† In situ hybridization(ISH) assay for Epstein–Barr virus encoded RNA (EBER) in the tissue specimen.

‡ EBV titer in blood at time of disease diagnosis, No FU=no follow-up for EBV titer.

§ Lost to follow-up, "− " = no, "+" = yes.

TABLE 2. Summary of the Clinical Characteristics in 12 Patients With Posttransplantation Lymphoproliferative Disorder of the Thorax

Characteristics		Patient (n = 12)
Age, Median (range, months)	Diagnosis*	46(34–68)
	Transplantation†	40(28–68)
	Time before PTLD‡	49(2–128)
Onset	Early onset(<1 year)	4(33.3)
	Late onset(≥1 year)	8(66.7)
Smoker	Yes	1(8.3)
	No	11(91.7)
Transplant	Liver	4
	Kidney	5
	Kidney and pancreas	1
	Heart	1
	Bone marrow	1
	Lung	0
Histologic subtype	Monomorphic	11(91.7)
	Nonmonomorphic	1(8.3)
Histologic cell type	Diffuse large B-cell type	8(66.7)
	Plasmacytoma	1(8.3)
	Peripheral T-cell type, not otherwise specified	2(16.7)
	Polymorphic	1(8.3)
PTLD within the organ allograft	Yes	1(8.3)
	No	11(91.7)
EBV-encoded RNA status (tissue specimen)	Positive	10(83.3)
	Negative	2(16.7)
EBV PCR (blood)	Positive	8(66.7)
	Negative	4(33.3)
Seroconversion	Yes	3
	No§	9
	No follow-up for EBV titer	6
Clinical symptom	Asymptomatic	7(58.3)
	Fever	4(33.3)
	Palpable neck mass	1(8.3)
Initial therapy	Surgery	3
	Reduced immunosuppresion	11
	Chemotherapy	11
Chemotherapeutic regimen	R-CHOP	7
	CHOP	3
	Rituximab	1
Response to treatment	CR	7(58.3)
	PR	4(33.3)
	PD	0(0)
	Undeterminated‖	1(8.3)

CHOP = cyclophosphamide, doxorubicine, vincristine, and prednisolone, CR = Complete remission, EBV = Epstein–Barr virus, PCR = polymer-polymerase chain reaction, PD = Progressive disease, PR = Partial remission, R-CHOP = rituximab, cyclophosphamide, doxorubicine, vincristine, and prednisolone.

* Median age when the patient received the diagnosis of PTLD.

† Median age when the patient had the organ or bone marrow transplantation.

‡ Median time between transplantation and the development of PTLD, Data are presented as median (range), mean ± standard deviation or No. (%), unless otherwise indicated.

§ None patients did not undergo a EBV PCR before diagnosis of PTLD.

‖ Lost to follow-up.

Statistical Analysis

All the values are given as medians (range), means ± standstandard deviations for continuous variables, and frequencies and percentages for categorical variables. Statistical analysis was performed using a commercial statistical software package (SPSS for Windows, version 21.0, SPSS, Chicago, IL) by a statistician with 10-year experience (no author).

RESULTS

Patient Characteristics

The median age of the patients at the PTLD diagnosis was 46 years (range, 34–68). The median time between the transplantation and the PTLD onset was 49 months (range, 2–128).

Four patients presented with PTLD within the first 12 months after transplantation, which is called ''early-onset'' PTLD, and 8 patients presented with late-onset PTLD (>12 months after transplantation). Of the 12 PTLD patients, 1 (8.3%) was polymorphic and 11 (91.7%) was monomorphic; there were 8 cases of diffuse large B-cell lymphoma, 2 cases of peripheral T-cell lymphoma, not otherwise unspecified (PTCL, NOS), and a case of plasmacytoma. Twelve patients underwent in situ hybridization for EBER, and 10 of them showed positive signals in their tumor cell nuclei (Figures 2–4).

Also, all the patients underwent an EBV PCR test of their blood at the time of their diagnosis. Among them, 8 cases had positive results and 3 cases had already been subjected to routine EBV PCR monitoring for posttransplant surveillance, and these patients showed seroconversion without antiviral therapy.

The thoracic involvement was often asymptomatic (58.3%, 7/12), and the diagnosis was initially suspected according to the radiology imaging features in the routine check-up. The most common clinical symptom was fever (4/12) (Tables 1 and 2).

The chemotherapeutic regimens were R-CHOP (7/12; rituximab, cyclophosphamide, doxorubicine, vincristine, and prednisolone), CHOP (3/12; cyclophosphamide, doxorubicine, vincristine, and prednisolone), and rituximab only (1/12). The response to the treatment after the chemotherapy was complete remission (58.3%, 7/12) or partial remission (33.3%, 4/12). One patient's response was undetermined due to follow-up loss.

CT Evaluations

The most common CT pattern had LN involvement (10/12) (Figure 2). The detailed findings are shown in Tables 3 and 4. The median size of the involved LNs was 13 mm (range, 7–34). Of the 10 patients, 9 showed iso-attenuations, and all revealed homogenous attenuation, 9 multiple lesions, and 6 bilateral lesions. Abdominal lymphadenopathy was seen in 8 patients.

Regarding the lung involvement, 4 consolidative masses and 11 ill-defined nodules or nodular consolidations were identified in 3 patients (Figures 4–6). Only 1 lesion showed necrotic lower attenuation (Figure 5). The median size of the lung lesion was 11 mm (range, 6–76). The most frequently involved lobe was the right upper lobe (73.3%, 11/15) (Figures 4 and 6). Three patients with lung lesions had multiple lesions (Tables 3 and 4, and Figure 5). Of the 15 lung lesions, 13 showed iso-attenuation, and all showed homogenous attenuation.

TABLE 3. Summary of the CT Characteristics in 12 Patients with Posttransplantation Lymphoproliferative Disorder of the Thorax and FDG-PET Characteristics in 10 Patients

CT Patterns*	Patient (n = 12)*
Lymph node involvement	10
Location	
Supraclavicular area	3
Mediastinum	7
Axilla	4
Laterality	
Unilateral	4
Bilateral	6
Lung involvement	3
Pleural effusion	4
Unilateral	3
Bilateral	1
FDG-PET, SUVmax	Patient (n = 10)
Median (range)	7.7(2.7–25.5)

Data are presented as median (range). CT = computed tomography, FDG-PET = F-18 fluoro-2-deoxy-D-glucose positron emission tomographic, SUVmax = maximum-standardized uptake value.
* The numbers are not mutually exclusive.

Pleural involvement appeared as pleural effusion (33.3%, 4/12); and among the patients, three had unilateral pleural effusion (Figure 3). Pleural involvement was concurrent with any other lesion as the LN (3/12) and the lung (1/12) involvement. There was no single imaging finding of isolated pleural involvement.

FDG-PET Evaluations

On the FDG-PET scans, the SUVmax of all the involved lesions was hypermetabolic (median, 7.7 and range, 2.7–25.5) (Table 3).

DISCUSSION

PTLD is a well-recognized complication of solid organ transplants and hematopoietic stem cell transplantation.[7] Although relatively uncommon, it is important because it can be fatal. Because the radiologic findings of PTLD are generally nonspecific, the radiologic features of PTLD are not yet well-established. In this study, we elucidated the CT and PET-CT findings of 12 patients with PTLD, focused on the thoracic involvement.

The CT features of thoracic PTLD were a large nodal mass and clusters of normal-sized LNs in the hilum, mediastinum, supraclavicular, cervical, and axillary areas. Lung involvement was relatively rare. Most of the LNs had a bilateral location and iso-attenuation and homogenous attenuation compared to the adjacent muscle. Necrosis was very rare, despite a large solitary nodal mass. In this study, combined abdominal lymphadenopathy was also common. These imaging findings are the same as those of lymphoma without a history of transplantation, which frequently appears as lymphadenopathy or occasionally, as a lung nodule or mass.[8,9] Differential diagnoses include bacterial, fungal, or mycobacterial infection in the immunocompromised patient, which frequently appears as extensive airspace consolidation or a centrilobular or interstitial nodule of the lung. LN involvement is relatively rare in these infections. Primary or

TABLE 4. Detailed CT Characteristics in 12 Patients With Posttransplantation Lymphoproliferative Disorder of the Thorax

Patient No./ Age (year)/ Sex	Patterns	Laterality	Size of Prominent LN, mm	Location of LN	Size of Lung Lesion, mm	Attenuation	Heterogeneity	Number of Lesions
1/35/M	LN	Unilateral	7	Supraclavicular		Iso	Homo	4
2/60/M	Lung				76	Iso	Homo (with necrosis)	3
	Lung				7	Hyper	Homo	
	Lung				6	Iso	Homo	
	LN	Unilateral	10	Mediastinum		Iso	Homo	12
3/40/M	LN	Bilateral	10	Supraclavicular, axilla, mediastinum, and hilum		Iso	Homo	13
4/44/M	LN	Bilateral	17	Supraclavicular, and mediastinum,		Hypo	Homo	14
5/35/F	Lung				46	Iso	Homo	10
	Lung				26	Iso	Homo	
	Lung				14	Iso	Homo	
	Lung				7	Iso	Homo	
	Lung				7	Iso	Homo	
	Lung				7	Iso	Homo	
	Lung				77	Iso	Homo	
	Lung				57	Iso	Homo	
	Lung				6	Iso	Homo	
	Lung				7	Hypo	Homo	
6/54/F	LN	Bilateral	12	Axilla, Mediastinum		Iso	Homo	7
7/62/F	LN	Bilateral	17	Axilla, and Mediastinum,		Iso	Homo	14
8/48/M	LN	Bilateral	16	Mediastinum		Iso	Homo	6
9/34/M	LN	Unilateral	14	Mediastinum		Iso	Homo	2
10/68/M	Lung				11	Iso	Homo	2
	Lung				21	Iso	Homo	
11/44/M	LN	Bilateral	10	Axilla, and Mediastinum		Iso	Homo	3
12/54/M	LN	Unilateral	34	Axilla		Iso	Homo	1

Homo = homogeneous, Hyper = hyperattenuation, Hypo = hypoattenuation, Iso = isoattenuation, LLL = left lower lobe, LN = lymph node, RLL = right lower lobe, RUL = right upper lobe.

secondary malignancy usually shows asymmetric and unilateral lymphadenopathy, and heterogeneous attenuation with frequent necrotic attenuation.

Previous studies have investigated the use of FDG-PET in PTLD.[10,11] In the current study, all the involved lesions in the 10 patients revealed hypermetabolism on the FDG-PET. These results support the diagnosis of PTLD. FDG-PET is important for evaluating the systemic involvement of PTLD and intrathoracic lymphoma.[12,13]

Approximately 50% to 70% of all PTLD cases are related to EBV infection.[14] Activated T-cells suppress propagation and eliminate EBV-infected B cells, whereas T-cell function is impaired in immunocompromised subjects, which may result in uncontrolled proliferation of EBV-transformed B-cells.[15] Studies on the predictive role of the host EBV DNA (peripheral blood) in the risk of PTLD have shown conflicting results.[16,17] This may be due to the differences in the patient populations studied with respect to age and the EBV serostatus at the time of the transplant. The British guideline on the routine surveillance of adult transplantation populations for EBV DNAemia via PCR does not recommend this outside the hematopoietic stem cell transplantation population,[18] whereas the American Society of Transplantation recommends posttransplant EBV viral load surveillance monthly for a year in EBV-seronegative recipients after solid organ transplantation.[17] In this study, only 3 patients underwent routine surveillance, and they showed seroconversion. Two patients had EBV-negative PTLD. The awareness of EBV-negative PTLD has increased over the past decade. The features of EBV-negative PTLD are known as late onset and poorer response to therapy.[19,20] Additionally, it has been shown to be more frequently monomorphic than EBV-positive PTLD.[19]

The incidence of PTLD is very low in our population compared with that in previous studies that reported the incidence of PTLD as 1% to 10%.[18] It is well known that the development of PTLD is closely related to the degree and level of immunosuppressive therapy. It has been shown that PTLD occurs at a much higher rate (ie, 10%–25%) in solid

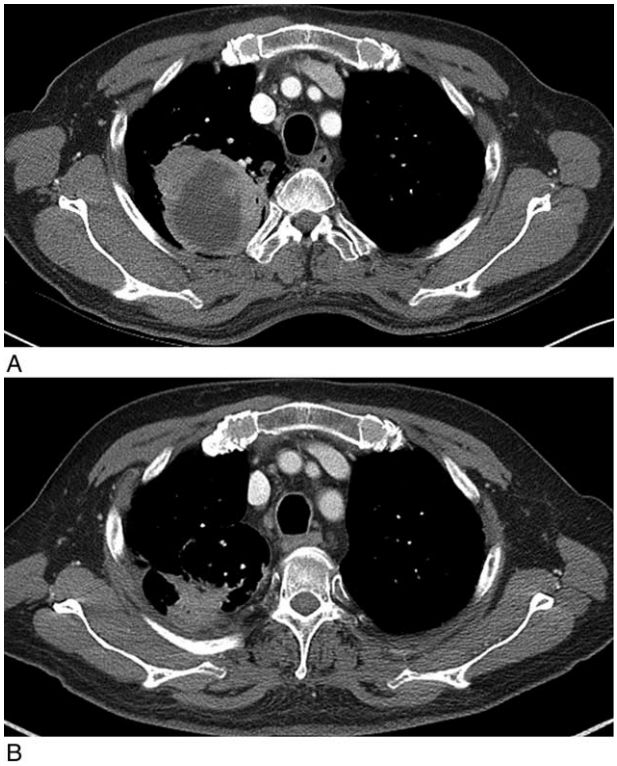

FIGURE 5. A 61-year-old man who developed PTLD of the thorax a year and 2 months after liver transplantation (patient 2). (A) Contrast-enhanced axial CT image obtained at the level of the aortic arch vessel showing a 68 mm mass-like airspace consolidation with central, large, and necrotic lower attenuation in the right upper lobe. Microscopically, the tumor showed monomorphic PTLD of the diffuse large B-cell type (not shown). (B) Follow-up CT scan obtained 9 months later showing partial resolution of the mass after immune therapy and chemotherapy. CT = computed tomography, PTLD = posttransplant lymphoproliferative disorder.

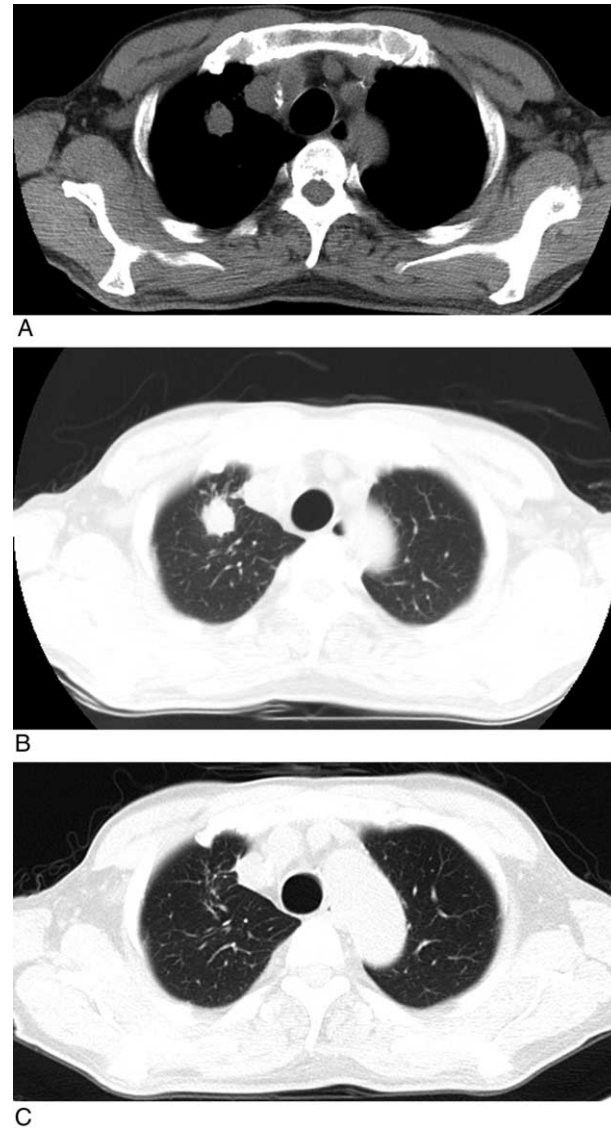

FIGURE 6. A 68-year-old man who developed PTLD of the thorax 7 months after liver transplantation (patient 10). (A, B) Nonenhanced axial CT mediastinal and lung window images obtained at the level of the aortic arch showing a 2 cm well-defined nodule in the right upper lobe. Microscopically, the tumor showed monomorphic PTLD of the diffuse large B-cell type (not shown). (C) Follow-up CT scan obtained 8 months later showing complete resolution of the mass after immune therapy and chemotherapy (not shown). CT = computed tomography, PTLD = posttransplant lymphoproliferative disorder.

organ transplants that require a higher degree of immunosuppression, such as the heart and lung, but the incidence rates are much lower (ie, 1%–5%) with transplants with lower immune suppression dosing such as the kidney or liver.[7] The majority of our patients (82.1%, 6571/8000) were kidney or liver transplant recipients. In addition, our center did not tend to use antithymocyte globulin or Orthoclone OKT3 for induction therapy, as they are known to be associated with an increased risk of PTLD.

This study had several limitations. The most significant of these was that our analysis was conducted at a single referral center with a small number of patients. Moreover, the monitoring of the CT or EBV surveillance was based on the decision of the attending physician for each transplant program. Finally, the type of transplant, and accordingly, the level of immunosuppression, was diverse in the patients in this study. These factors might have resulted in the CT and PET-CT findings.

In conclusion, in the patients with PTLD that involved the thorax, lymphadenopathy was the more common manifestation on the chest CT rather than lung involvement. The lesions showed hypermetabolism on the FDG-PET.

REFERENCES

1. Nalesnik MA, Jaffe R, Starzl TE, et al. The pathology of posttransplant lymphoproliferative disorders occurring in the setting of cyclosporine A-prednisone immunosuppression. *Am J Pathol.* 1988;133:173–192.
2. Nagington J, Gray J. Cyclosporin A immunosuppression, Epstein-Barr antibody, and lymphoma. *Lancet.* 1980;1:536–537.

3. Ho M, Jaffe R, Miller G, et al. The frequency of Epstein-Barr virus infection and associated lymphoproliferative syndrome after transplantation and its manifestations in children. *Transplantation.* 1988;45:719–727.
4. Murray JE, Wilson RE, Tilney NL, et al. Five years' experience in renal transplantation with immunosuppressive drugs: survival, function, complications, and the role of lymphocyte depletion by thoracic duct fistula. *Ann Surg.* 1968;168:416–435.
5. Nalesnik MA. Posttransplantation lymphoproliferative disorders (PTLD): current perspectives. *Semin Thorac Cardiovasc Surg.* 1996;8:139–148.
6. Lababede O, Meziane M, Rice T. Seventh edition of the cancer staging manual and stage grouping of lung cancer: quick reference chart and diagrams. *Chest.* 2011;139:183–189.
7. Jagadeesh D, Woda BA, Draper J, et al. Post transplant lymphoproliferative disorders: risk, classification, and therapeutic recommendations. *Curr Treat Opt Oncol.* 2012;13:122–136.
8. Lewis ER, Caskey CI, Fishman EK. Lymphoma of the lung: CT findings in 31 patients. *AJR Am J Roentgenol.* 1991;156:711–714.
9. Fishman EK, Kuhlman JE, Jones RJ. CT of lymphoma: spectrum of disease. *Radiographics.* 1991;11:647–669.
10. Panagiotidis E, Quigley AM, Pencharz D, et al. (18)F-fluorodeoxyglucose positron emission tomography/computed tomography in diagnosis of post-transplant lymphoproliferative disorder. *Leuk Lymphoma.* 2014;55:515–519.
11. Bianchi E, Pascual M, Nicod M, et al. Clinical usefulness of FDG-PET/CT scan imaging in the management of posttransplant lymphoproliferative disease. *Transplantation.* 2008;85:707–712.
12. Blaes AH, Cioc AM, Froelich JW, et al. Positron emission tomography scanning in the setting of post-transplant lymphoproliferative disorders. *Clin Transplant.* 2009;23:794–799.
13. Takehana CS, Twist CJ, Mosci C, et al. (18)F-FDG PET/CT in the management of patients with post-transplant lymphoproliferative disorder. *Nucl Med Commun.* 2014;35:276–281.
14. Nourse JP, Jones K, Gandhi MK. Epstein-Barr Virus-related post-transplant lymphoproliferative disorders: pathogenetic insights for targeted therapy. *Am J Transplant.* 2011;11:888–895.
15. Loren AW, Porter DL, Stadtmauer EA, et al. Post-transplant lymphoproliferative disorder: a review. *Bone Marrow Transplant.* 2003;31:145–155.
16. Schaffer K, Hassan J, Staines A, et al. Surveillance of Epstein-Barr virus loads in adult liver transplantation: associations with age, sex, posttransplant times, and transplant indications. *Liver Transplant.* 2011;17:1420–1426.
17. Humar A, Michaels M. American Society of Transplantation recommendations for screening, monitoring and reporting of infectious complications in immunosuppression trials in recipients of organ transplantation. *Am J Transplant.* 2006;6:262–274.
18. Parker A, Bowles K, Bradley JA, et al. Diagnosis of post-transplant lymphoproliferative disorder in solid organ transplant recipients – BCSH and BTS Guidelines. *Br J Haematol.* 2010;149:675–692.
19. Nelson BP, Nalesnik MA, Bahler DW, et al. Epstein-Barr virus-negative post-transplant lymphoproliferative disorders: a distinct entity? *Am J Surg Pathol.* 2000;24:375–385.
20. Leblond V, Davi F, Charlotte F, et al. Posttransplant lymphoproliferative disorders not associated with Epstein-Barr virus: a distinct entity? *J Clin Oncol.* 1998;16:2052–2059.